Chem. Mater. 1992, 4, 1246–1253

Low Molar Mass Liquid-Crystalline Glasses: Preparation and Properties of the α-(4-Cyanobiphenyl-4′-oxy)-ω-(1-pyreniminebenzylidene-4′-oxy)alkanes

G. S. Attard and C. T. Imrie*,†

Department of Chemistry, University of Southampton, Southampton, Hants SO9 5NH, U.K.

F. E. Karasz

Department of Polymer Science and Engineering, University of Massachusetts, Amherst, Massachusetts 01003

Received May 7, 1992. Revised Manuscript Received August 3, 1992

Ten members of the asymmetric dimer homologous series α-(4-cyanobiphenyl-4′-oxy)-ω-(1-pyreniminebenzylidene-4′-oxy)alkanes have been synthesized, and their mesogenic properties characterized. All the homologues exhibit glassy behavior, forming either nematic or smectic glasses, above room temperature. The thermal behavior of this series is discussed in detail, and the transitional properties of the homologues are compared to those of the related α,ω-bis(1-pyreniminebenzylidene-4′-oxy)alkanes and α,ω-bis(4-cyanobiphenyl-4′-oxy)alkanes dimer series. The differences between these series are interpreted in terms of changes in the anisometry of the molecular shape. The application potential of these novel materials is discussed briefly.

Introduction

Side-chain liquid-crystalline polymers have aroused considerable interest in recent years for they combine properties of macromolecules, for example, processibility and glassy behavior, with the electrooptic characteristics of low molar mass mesogens.[1] This combination of properties is at the root of many varied potential applications. One such application is optical information storage in which information is written onto a glassy mesophase by the local heating action of a laser.[2] This causes localized regions of the isotropic phase to form which, when the laser is switched off, are quenched into an isotropic glass phase. The coexistence of the two distinct textures, the scattering liquid-crystalline and the nonscattering isotropic textures, produces the required optical contrast. The vast majority of low molar mass mesogens are unsuited to such applications because either crystallization occurs resulting in the loss of optical contrast or, if room-temperature mesophases are employed in the device, the viscosity of the phase is too low to prevent the corruption of the information through molecular and/or collective motions. The incorporation of low molar mass anisotropic glasses into such devices, however, offers several advantages over the use of polymers. For example, monomers can be prepared in high purity with two major advantages: first, the reproducibility of transitional behavior is not a problem unlike that for side-chain polymers; second, the elimination of ionic impurities which in the polymers can lead to dielectric breakdown in the processing stage as well as limited device lifetimes. In addition, low molar mass materials are significantly easier to process using either electric or magnetic fields and device fabrication, in particular filling cells, could be achieved using existing technologies. Low molar mass glassy liquid crystals have been known for many years,[3] but typically these exhibit very low glass transition temperatures, well below room temperature. Also, to reveal the glassy phase, the sample often requires high quenching rates. An example of this is the extensively studied 4-methoxybenzylidene-4-butylaniline (MBBA) for which a glassy nematic phase can be achieved only by plunging the sample into liquid nitrogen. The T_g of this material is estimated to be approximately −14 °C.[4] Only in recent years have low molar mass mesogens with ambient T_g's been obtained.[5,6] These materials comprise molecules consisting of either naphthalene derivatives[6] or dimeric molecules linked laterally via sulfinyl or sulfonyl groups.[5] In a recent review, Wedler et al.[7] discussed certain aspects of structure–property relationships in low molar mass glassy mesogens and concluded that, in general, molecular features which enhance glassy behavior tend to suppress liquid crystallinity. To explore novel molecular architectures designed to exhibit glassy mesophases, Attard and Imrie[8] reported on the properties of the symmetric dimer series of the α,ω-bis(1-pyreniminebenzylidene-4′-oxy)alkanes (1), which were denoted by Py.O*n*O.Py in

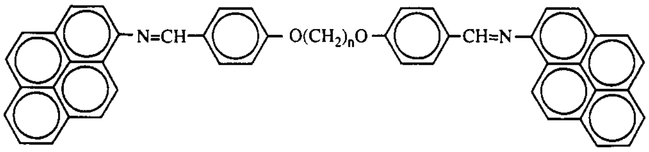

1

which *n* refers to the number of methylene units in the flexible alkyl core. The propyl homologue of this series exhibits an isotropic glassy phase with a T_g of 70 °C and the butyl homologue a nematic glass with a T_g of 66 °C. The hexyl, octyl, and decyl homologues form smectic

---

* To whom correspondence should be addressed.

† Permanent address: Department of Chemistry, University of Aberdeen, Meston Walk, Old Aberdeen AB9 2UE, Scotland.

[1] Attard, G. S. *High Value Polymers*; Fawcett, A. H., Ed.; Royal Society of Chemistry: London, 1991; p 131.

[2] McArdle, C. B. In *Side Chain Liquid Crystal Polymers*; McArdle, C. B., Ed.; Blackie and Son: Glasgow, 1989; Chapter 13.

[3] Tsuji, K.; Sorai, M.; Seki, S. *Bull. Chem. Soc. Jpn.* **1971**, *44*, 1452.

[4] Lydon, J. E.; Kessler, J. O. *J. Phys.* (*Les Ulis*) **1975**, *36*, C1-153.

[5] Dehne, H.; Roger, A.; Demus, D.; Diele, S.; Kresse, H.; Pelzl, G.; Wedler, W.; Weissflog, W. *Liq. Cryst.* **1989**, *6*, 47.

[6] Schäfer, W.; Uhlig, G.; Zaschke, H.; Demus, D.; Diele, S.; Kresse, H.; Ernst, S.; Wedler, W. *Mol. Cryst. Liq. Cryst.* **1990**, *191*, 269.

[7] Wedler, W.; Demus, D.; Zaschke, H.; Mohr, K.; Schäfer, W.; Weissflog, W. *J. Mater. Chem.* **1991**, *1*, 347.

[8] Attard, G. S.; Imrie, C. T. *Liq. Cryst.* **1992**, *11*, 785.

0897-4756/92/2804-1246$03.00/0

Scheme I

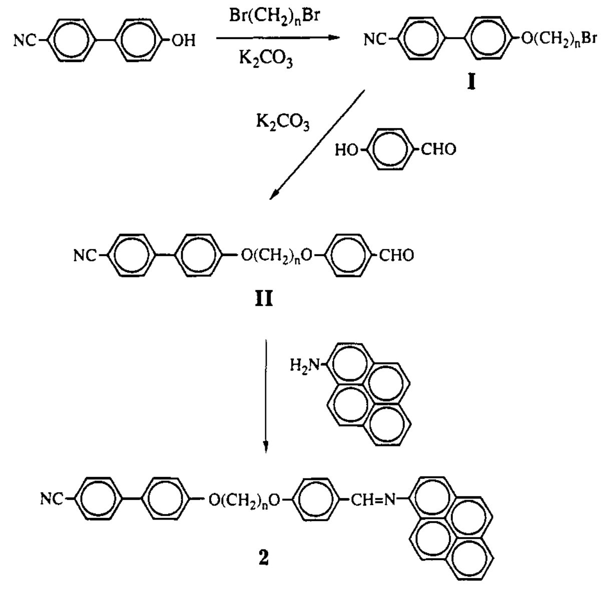

glasses, while the remaining members with the exception of the pentyl homologue, exhibit nematic glasses. The T_g's decrease from 66 °C for the hexyl homologue to 35 °C for the dodecyl homologue and the glassy behavior of these materials was attributed to the pyrene–pyrene interactions. Therefore, these materials demonstrate the ability of pyrene-containing moieties to exhibit glassy behavior. They do not exhibit, however, the correct dielectric anisotropy to be useful in device applications in which it is required that the director should reorient parallel to an aligning electric field. Recently, a new class of liquid crystals has been described, asymmetric dimeric liquid crystals in which two differing mesogenic units are linked by a flexible alkyl spacer[9] and as part of a continuing program to develop prototype materials for advanced electrooptic technologies, we have combined the glassy behavior of pyrene with the desirable electrooptic characteristics of cyanobiphenyl by synthesizing the α-(4-cyanobiphenyl-4′-oxy)-ω-(1-pyreniminebenzylidene-4′-oxy)alkanes (**2**).

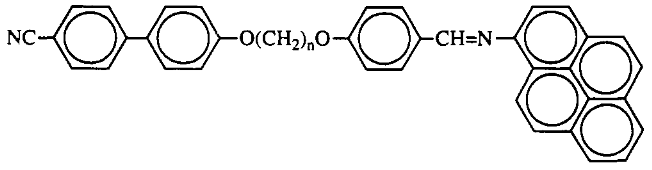

2

These are denoted by the acronym CBO*n*O.Py, where *n* refers to the number of methylene units in the flexible alkyl core. The CBO*n*O.Py series does indeed contain anisotropic glasses, and we describe their thermal behavior in detail. We compare also their transitional properties with those of the symmetric dimers, the Py.O*n*O.Py series discussed already, and the symmetric α,ω-bis(4-cyanobiphenyl-4′-oxy)alkanes (**3**), denoted by BCBO*n*.[10]

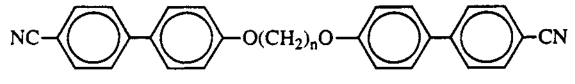

3

Table I. Analytical Data for 1-Bromo-7-(4-cyanobiphenyl-4′-oxy)heptane

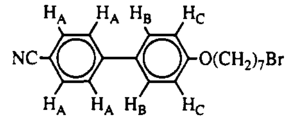

4

^{1}H NMR (CDCl$_3$, TMS, δ, ppm)[12] 7.69, 7.64 (overlapping d, 4 H, H_A), 7.53 (d, 2 H, H_B), 6.99 (d, 2 H, H_C), 4.00 (t, 2 H, CH_2O), 3.43 (t, 2 H, CH_2Br), 1.88 (m, 4 H, CH_2CH_2O, CH_2CH_2Br), 1.49 (m, 6 H, $CH_2CH_2CH_2$)

IR (Nujol mull) 2222 cm^{-1} (CN stretch)

λ_{max}(CH$_2$Cl$_2$) 297 nm.

Anal. Calcd for $C_{20}H_{22}BrNO$: C, 64.52; H, 5.96; Br, 21.46; N, 3.76. Found: C, 64.88; H, 6.04; Br, 21.42; N, 3.59.

Table II. Analytical Data for 1-(4-Cyanobiphenyl-4′-oxy)-7-(4-formylphenyl-4′-oxy)heptane

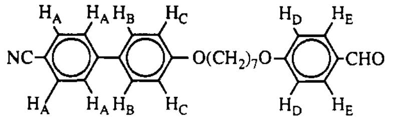

5

^{1}H NMR (CDCl$_3$, TMS, δ, ppm)[12] 9.88 (s, CHO, 1 H), 7.83 (d, 2 H, H_E), 7.69, 7.64 (overlapping d, 4 H, H_A), 7.53 (d, 2 H, H_B), 6.99 (d, 4 H, H_CH_D), 4.05, 4.02 (overlapping t, 4 H, CH_2O), 1.84 (m, 4 H, CH_2CH_2O), 1.49 (m, 6 H, $CH_2CH_2CH_2$)

IR (Nujol mull) 2221 (CN stretch), 1686 cm^{-1} (C=O stretch)

λ_{max}(CH$_2$Cl$_2$) 292 nm

Anal. Calcd for $C_{27}H_{27}NO_3$: C, 78.42; H, 6.58; N, 3.39. Found: C, 78.01; H, 6.58; N, 3.54.

Experimental Section

Synthesis. The synthetic route used for the preparation of the CBO*n*O.Py series is shown in Scheme I; the average overall yield over the three steps was approximately 42%.

α-Bromo-ω-(4-cyanobiphenyl-4′-oxy)alkanes, I. The α-bromo-ω-(4-cyanobiphenyl-4′-oxy)alkanes were prepared by the reaction of 4-cyano-4′-hydroxybiphenyl with a large excess of a dibromoalkane in dry acetone with potassium carbonate as base according to a procedure described by Crivello et al.[11] Thus for 1-bromo-7-(4-cyanobiphenyl-4′-oxy)heptane, 4-cyano-4′-hydroxybiphenyl (2.5 g, 12.8 mmol), 1,7-dibromoheptane (38.5 g, 128 mmol) and anhydrous potassium carbonate (13.3 g, 96 mmol) were added to dry acetone (250 mL), and the reaction mixture was refluxed with stirring for 24 h. The reaction mixture was filtered and the inorganic residues were washed thoroughly with acetone. The filtrates were combined and the acetone was removed in a rotary evaporator. The reaction mixture was poured into cooled petroleum ether (350 mL). After several hours the resulting white precipitate was filtered off and washed thoroughly with petroleum ether. The crude product was recrystallized twice from aqueous ethanol with hot filtration to yield 3.7 g (70%) of white crystals. The hot filtrations ensured the complete removal of the dimeric side product, 1,7-bis(4-cyanobiphenyl-4′-oxy)heptane, which is essentially insoluble in ethanol. Table I lists the analytical data for 1-bromo-7-(4-cyanobiphenyl-4′-oxy)heptane.

α-(4-Cyanobiphenyl-4′-oxy)-ω-(4-formylphenyl-4′-oxy)alkanes, II. The α-(4-cyanobiphenyl-4′-oxy)-ω-(4-formylphenyl-4′-oxy)alkanes were prepared by the reaction of an α-bromo-ω-(4-cyanobiphenyl-4′-oxy)alkane with 4-hydroxybenzaldehyde using potassium carbonate as base in dimethylformamide. Thus for 1-(4-cyanobiphenyl-4′-oxy)-7-(4-formylphenyl-4′-oxy)heptane, 1-bromo-7-(4-cyanobiphenyl-4′-oxy)heptane (3 g, 8 mmol), 4-hydroxybenzaldehyde (1.2 g, 9.8 mmol), and anhydrous potassium carbonate (5.5 g, 40 mmol) in dimethylformamide (20 mL) were

---

(9) Hogan, J. L.; Imrie, C. T.; Luckhurst, G. R. *Liq. Cryst.* **1988**, *3*, 645. Attard, G. S.; Garnett, S.; Hickman, C. G.; Imrie, C. T.; Taylor, L. *Liq. Cryst.* **1990**, *7*, 495.

(10) Emsley, J. W.; Luckhurst, G. R.; Shilstone, G. N.; Sage, I. *Mol. Cryst. Liq. Cryst. Lett.* **1984**, *102*, 223.

(11) Crivello, J. V.; Deptolla, M.; Ringsdorf, H. *Liq. Cryst.* **1988**, *3*, 235.

(12) This analysis treats the aromatic regions as if they were a simple spin–spin system. This however is not the case, and the assignment of the peaks as doublets is not strictly correct.

Table III. Transition Temperatures and Entropies of Transition for the α-(4-Cyanobiphenyl-4'-oxy)-ω-(1-pyreniminobenzylidene-4'-oxy)alkanes

n	T_{C-}/°C	T_g/°C	T_{SN}/°C	T_{NI}/°C	$\Delta S_{C-}/R$	$\Delta S_{SN}/R$	$\Delta S_{NI}/R$
3	199	51		120	11.77		0.07
4	217	54	117[a]	233	12.33	0.09[a]	0.58
5	152	41	50	154	2.45	0.03	0.17
6	172	41	116[a]	208	10.70	0.69[a]	0.86
7	156	37	65	164	11.50	0.29	0.28
8	154	33	108	193	11.14	0.06	0.99
9	153	33	55	161	14.50	0.03	0.32
10	172	30	84[a]	179	17.80	0.06[a]	1.07
11	150	34		159	18.20		0.50
12	160	29	63[b]	169	12.34		0.94

[a] Data from cooling run. [b] Measured using microscope.

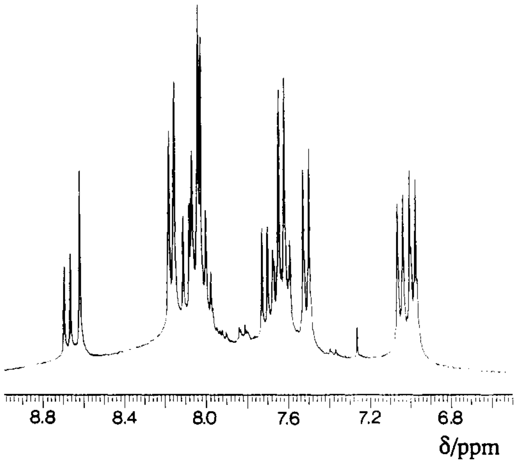

Figure 1. Aromatic region of the ^{1}H NMR spectrum of CBO7O.Py.

refluxed with stirring for 4 h. The reaction mixture was allowed to cool and poured into water (250 mL). The resulting precipitate was filtered off and recrystallized twice from aqueous ethanol to yield 2.5 g (75%) of pale yellow crystals. The analytical data for the final product are listed in Table II.

α-(4-Cyanobiphenyl-4'-oxy)-ω-(1-pyreniminebenzylidene-4'-oxy)alkanes, 2. The α-(4-cyanobiphenyl-4'-oxy)-ω-(1-pyreniminebenzylidene-4'-oxy)alkanes were prepared by the condensation reaction of an α-(4-cyanobiphenyl-4'-oxy)-ω-(4-formylphenyl-4'-oxy)alkane with 1-aminopyrene. Thus for 1-(4-cyanobiphenyl-4'-oxy)-7-(1-pyreniminebenzylidene-4'-oxy)heptane, 1-(4-cyanobiphenyl-4'-oxy)-7-(4-formylphenyl-4'-oxy)heptane (1.5 g, 3.6 mmol) was dissolved in hot absolute ethanol (50 mL). To this solution was added 1-aminopyrene (1.0 g, 4.6 mmol) and a few crystals of *p*-toluenesulfonic acid. The reaction mixture was refluxed with stirring for 3 h and then allowed to cool. The resulting solid was filtered off and recrystallized twice from a chloroform/absolute ethanol mixture to yield 1.8 g (80%) of yellow crystals. The aromatic region of the ^{1}H NMR spectrum of this compound is very complex and thus is shown as Figure 1.

^{1}H NMR ($CDCl_3$, TMS, δ, ppm) 8.62 (s, 1 H, CH=N), 4.07, 4.01 (overlapping t, 4 H, CH_2O), 1.84 (m, 4 H, CH_2CH_2O), 1.51 (m, 6 H, $CH_2CH_2CH_2$). IR (Nujol mull) 2223 cm^{-1} (CN stretch). Anal. Calcd for $C_{43}H_{36}N_2O_2$: C, 84.28; H, 5.92; N, 4.57. Found: C, 84.21; H, 6.03; N, 4.57.

Characterization. The proposed structures of the final products and their intermediates were verified by ^{1}H NMR spectroscopy using a Varian XL-300 NMR spectrometer and IR spectroscopy using an IBM System 9000 FT-IR spectrometer together with elemental analysis performed by the University of Massachusetts Microanalytical Laboratory. The high purity of the products was checked by thin-layer chromatography. The UV-vis spectra of the compounds were recorded using a Perkin-Elmer Lambda 9 UV-vis-NIR spectrophotometer interfaced to a Perkin-Elmer Laboratory computer.

Thermal Characterization. The transitional properties of the CBO*n*O.Py dimers were investigated by differential scanning calorimetry using a Perkin-Elmer DSC-7 which had been calibrated using indium as standard. For each compound two samples were run and the results listed are the averaged values. The heating and cooling rates employed in the experiments are discussed later. The optical textures of the phases exhibited by these compounds were studied by polarizing light microscopy using a Zeiss polarizing light microscope equipped with a Linkam heating stage.

Results and Discussion

Thermal Behavior. The transitional properties of the CBO*n*O.Py dimers are listed in Table III. The melting points and the liquid-crystalline transition temperatures given are the peak maxima in the DSC traces. The glass transition temperatures quoted are the inflection points in the baseline. With the exceptions of the hexyl and undecyl homologues, each sample was treated in an identical manner, namely, heated at 10 °C min^{-1} into the isotropic phase, then cooled to −30 °C at 10 °C min^{-1}, held at that temperature, and subsequently reheated into the isotropic phase. The hexyl and undecyl homologues required quenching in order to reveal glassy behavior. All the members exhibit enantiotropic nematic behavior with the exception of the propyl homologue for which a monotropic nematic phase is observed. The nematic phase was assigned on the basis of the optical textures when viewed through the polarizing microscope, a schlieren texture which flashed when subjected to mechanical stress being observed for each compound. In addition to nematic behavior a monotropic smectic phase is observed for each compound with the exceptions of the propyl and undecyl members. The smectic–nematic transition could not be detected using DSC for the dodecyl member. On cooling the nematic phases for the even-membered compounds, the optical textures when viewed through the polarizing microscope changed to give regions of focal conic fans and homeotropic textures. Consequently, this lower temperature phase is assigned as a smectic A phase. In contrast, the optical textures for the odd-membered compounds remained unchanged on cooling to room temperature. No indication of a smectic–nematic transition was observed either optically or in the DSC trace for CBO3O.Py, and so we assume this compound is purely nematogenic. However, the DSC trace of the pentyl homologue does contain a second transition, and this is assigned as a smectic–nematic transition. On cooling the nematic phases of the heptyl and nonyl homologues at 10 °C min^{-1}, no textural changes occur, but on annealing at 60 and 50 °C, respectively, focal conic fan textures do develop. The transition temperatures measured using the microscope for the smectic–nematic transition in both odd- and even-membered compounds agree well with the weak first-order transitions observed in the DSC traces. No evidence of a smectic–nematic transition was found either by DSC or polarizing light microscopy for the undecyl homologue, although this sample did have a tendency to

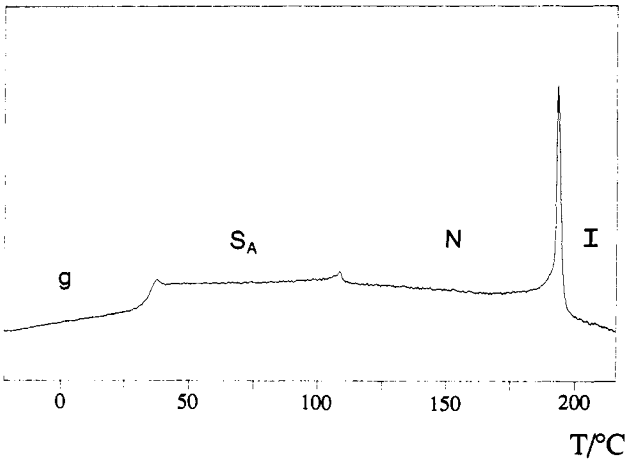

Figure 2. DSC trace for the second heating cycle of CBO8O.Py.

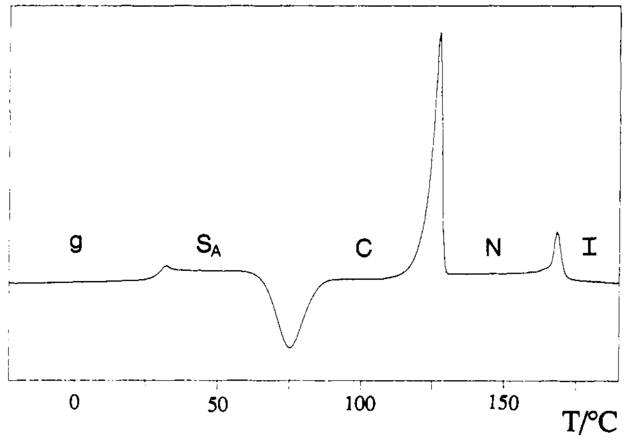

Figure 3. DSC trace for the second heating cycle of CBO12O.Py.

crystallize on cooling. The lack of textural change at the smectic to nematic transition for the pentyl, heptyl, and nonyl homologues results from the close proximity of the glass transition as well as the small entropy changes associated with the transition. This is often a problem in the phase identification for side-chain liquid-crystalline polymers[13] but is unusual for low molar mass mesogens. However, it is reasonable to assume that the deviation from thermodynamic equilibrium which is characteristic of polymeric glass-forming systems also occurs in the dimers we have synthesized.

At a cooling rate of 10 °C min^{-1} the compounds form a glassy liquid-crystalline phase with the exceptions of the hexyl and undecyl homologues which required quenching at 50 °C min^{-1} in order to reveal glassy behavior. The homologues exhibit one of two types of behavior on reheating at 10 °C min^{-1} from −30 °C. The propyl and octyl homologues exhibit no recrystallization on reheating; a typical DSC trace for the octyl homologue is shown in Figure 2. Three transitions are clearly evident: first, a second-order transition corresponding to the glass transition; second, a weak first-order transition, the smectic–nematic transition, and finally, a stronger first-order transition, the nematic–isotropic transition. The remaining compounds all exhibit cold crystallization on heating. This can be seen in the DSC trace for the dodecyl member shown in Figure 3, in which the glass transition is followed by an exothermic crystallization peak. At higher temperatures the melting peak is evident as a strong first-order transition followed by the weaker first-order nematic–isotropic transition. This tendency to crystallize does not necessarily limit the application potential of these materials, as will be discussed later, and furthermore the stability of the glassy phases at room temperature is excellent.

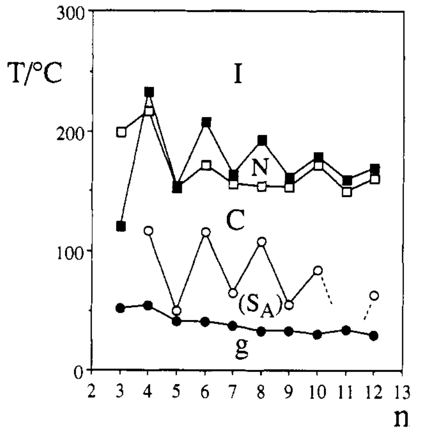

Figure 4. Dependence of the transition temperatures on the number of methylene units *n* in the flexible spacer for the CBO*n*O.Py homologous series. Melting points are denoted by □, ■ indicates nematic–isotropic transitions, ● glass transitions and ○ smectic–nematic transitions.

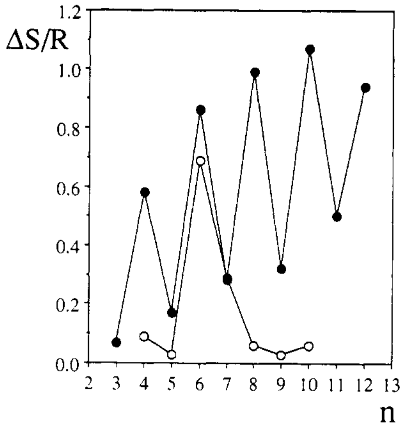

Figure 5. Dependence of the entropies associated with the nematic–isotropic transition, denoted by ●, and for the smectic–nematic transition, ○, on the number of methylene units in the flexible spacer for the CBO*n*O.Py series.

The dependence of the transition temperatures on the number of methylene units *n* in the flexible spacer for the CBO*n*O.Py series is shown as Figure 4. With the exception of the octyl homologue, the melting points exhibit a regular alternation on increasing *n* with the even-membered spacers having the higher values. The clearing points and the smectic–nematic transition temperatures show a dramatic odd–even effect on varying chain length; this is a characteristic feature of dimeric liquid crystals.[14] It is interesting to note that whereas the alternation of the clearing points attenuates quickly, that exhibited by the smectic–nematic transition temperatures does not. By contrast, the glass transition temperatures show little dependence on the parity of *n* and tend to decrease slowly on increasing the spacer length.

Figure 5 shows the dependence of the entropy changes associated with the clearing point and the smectic–nematic transition on the number of methylene units in the flexible spacer. The clearing entropies exhibit a pronounced odd–even effect, and this again is typical behavior for

---

(13) McRoberts, A. M.; Denman, R.; Gray, G. W.; Scrowston, R. M. *Makromol. Chem., Rapid Commun.* **1990**, *11*, 617.

(14) Date, R. W.; Imrie, C. T.; Luckhurst, G. R.; Seddon, J. M. *Liq. Cryst.* **1992**, *12*, 203.

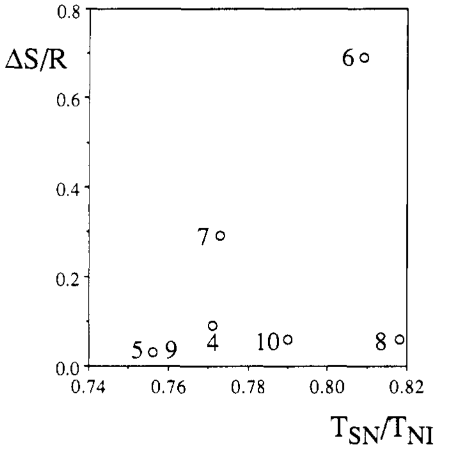

Figure 6. Entropies associated with the smectic–nematic transition as a function of the McMillan parameter for the CBO*n*O.Py series.

dimeric liquid crystals.[14] This large alternation has been interpreted recently in terms of the alternation in the long-range orientational order,[14] and this appears to be supported by the alternation found for the second rank order parameter for the long axis of the cyanobiphenyl group of the BCBO*n* series.[15] By contrast to this largely anticipated behavior, the entropy changes associated with the smectic–nematic transition exhibit a more unusual dependence on *n*, in that the hexyl and heptyl homologues show much larger values than the other members of the series. This can be seen also in Figure 6, which shows the dependence of the entropy of transition on the McMillan parameter, which is the ratio of transition temperatures T_{S_AN}/T_{NI}. McMillan theory predicts that the transitional entropy, $\Delta s_{S_AN}/R$, should decrease as the nematic range increases, i.e., as T_{S_AN}/T_{NI} decreases, until a tricritical point is reached at which the transition becomes second order.[16] It has been shown that symmetric dimeric liquid crystals behave as this theory predicts even though it was developed for rigid molecules with cylindrical symmetry.[14] More surprisingly it was shown that dimers with even- and odd-membered spacers behave similarly at this transition quite unlike the dramatic alternation associated with the clearing transition. Figure 6 reveals that for the CBO*n*O.Py series not only do the hexyl and heptyl homologues exhibit strongly first-order transitions but the remaining members show transitions which are first order, albeit weakly, implying a very low tricritical temperature for this system. Indeed, McMillan theory is unable to predict such a low temperature. The molecular significance of these observations is unclear but may suggest that the structure of the smectic A phase is unusual. Asymmetric dimers in which a specific interaction occurs between the differing units have been shown to exhibit an intercalated smectic A phase in which the differing units overlap and as a result, the entropy of transition tends to be higher than anticipated.[9] Obviously the stability of such a phase depends, in part, on the ability of the molecules to pack efficiently and so the spacer length is very important. It is possible that in this instance the packing efficiency is maximized for the hexyl member, hence the large entropy change. However, it is not apparent why this effect does not manifest itself in the temperatures of transition. Structural studies of these phases are planned in order to understand this behavior.

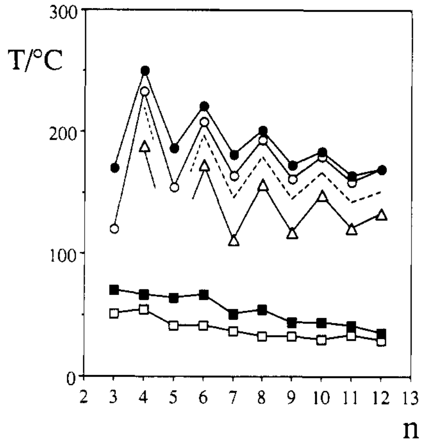

Figure 7. Comparison of the nematic–isotropic transition temperatures for the CBO*n*O.Py series ○, the BCBO*n* series ●, and the Py.O*n*O.Py series △. Also shown are the glass transition temperatures for the CBO*n*O.Py series, □, and for the Py.O*n*O.Py series, ■. The dashed line shows the mean values for the Py.O*n*O.Py and BCBO*n* series.

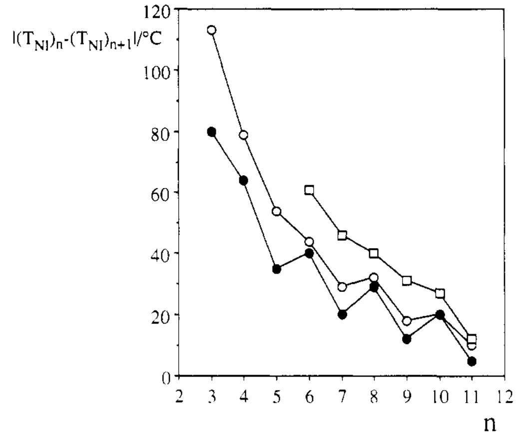

Figure 8. Comparison of the magnitude of the alternation in the nematic–isotropic transition temperatures on increasing the length of the flexible spacer for the BCBO*n* series, ●, the Py.O*n*O.Py series, □, and the CBO*n*O.Py series, ○.

Comparison of the CBO*n*O.Py, BCBO*n*, and Py.O*n*O.Py Series. Figure 7 compares the nematic–isotropic transition temperatures of the CBO*n*O.Py series with those of the parent symmetric dimers, the BCBO*n* and Py.O*n*O.Py series, and it is apparent that for any given value of *n* the transition temperatures are in the order

BCBO*n* > CBO*n*O.Py > Py.O*n*O.Py

The exceptions to this are BCBO12 and CBO12O.Py, for which the nematic–isotropic transition temperatures are equal. Figure 7 shows also the arithmetic mean of the transition temperatures for the symmetric dimers and it is very clear that all the members of the CBO*n*O.Py series exhibit T_{NI}'s which are greater than these mean values. If we assume that the core–core interactions are dominant in determining T_{NI}, then these results suggest that the mixed-core interaction is greater than the mean of the like-core interactions, i.e.

$$u_{AA}u_{BB}/u_{AB}^2 < 1$$

where the u_{ij}'s denote the strengths of the orientationally anisotropic interactions between the constituent mesogenic groups. Similar observations have been made for other asymmetric dimeric liquid crystals.[9] The nature of the mixed-core interaction will be discussed later. Figure 8 compares the magnitude of the alternation in the ne-

---

[15] Emsley, J. W.; Luckhurst, G. R.; Shilstone, G. N. *Mol. Phys.* **1984**, *53*, 1023.

[16] McMillan, W. L. *Phys. Rev. A* **1971**, *4*, 1238; *Ibid.* **1971**, *6*, 936.

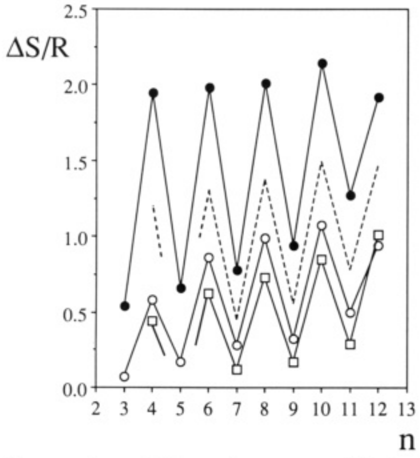

Figure 9. Comparison of the entropy associated with the nematic–isotropic transition for the CBO*n*O.Py series ○, the BCBO*n* series ●, and the Py.O*n*O.Py series □. The dashed line shows the mean values for the Py.O*n*O.Py and BCBO*n* series.

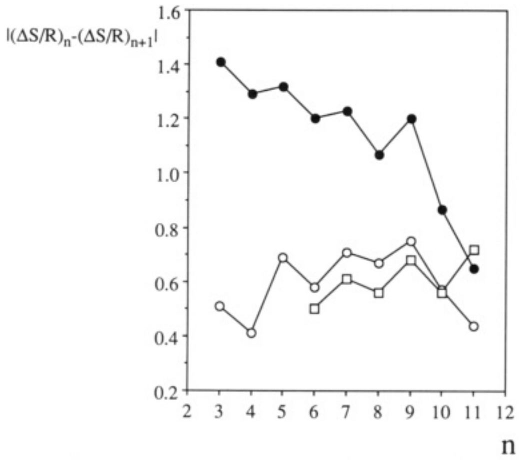

Figure 10. Comparison of the magnitude of the alternation in the entropy associated with the nematic–isotropic transition on increasing the length of the flexible spacer for the BCBO*n* series, ●, the Py.O*n*O.Py series, □, and the CBO*n*O.Py series, ○.

matic–isotropic transition temperatures for the three series by plotting $|(T_{NI})_n - (T_{NI})_{n+1}|$ as a function of n. This reveals that for the magnitude of alternation the order is

Py.O*n*O.Py > CBO*n*O.Py > BCBO*n*

The molecular significance of this reflects, in part, the increasing biaxiality of the molecule and this will be discussed in more detail later.

Figure 9 compares the nematic–isotropic transition entropy for the three series. For a given value of n, the entropy decreases in the order

BCBO*n* > CBO*n*O.Py > Py.O*n*O.Py

The exception to this is Py.O12O.Py, for which $\Delta S_{NI}/R$ is slightly greater than that of CBO12O.Py. Figure 9 shows also the arithmetic mean of the entropies exhibited by the symmetric series, and it is apparent that unlike the behavior exhibited by the T_{NI}'s, the transitional entropies for the CBO*n*O.Py series are consistently lower than the mean values. It should be stressed, however, that $\Delta S_{NI}/R$ for the even members of the CBO*n*O.Py series are considerably larger than those exhibited by either monomeric mesogens or side-chain liquid-crystal polymers. This almost certainly implies that the orientational ordering in the asymmetric dimers is larger; the relevance of this will be discussed later. Figure 10 shows the magnitude of the alternations in the nematic–isotropic entropies for the three series; for a given value of n the alternation is in the order

BCBO*n* > CBO*n*O.Py > Py.O*n*O.Py

The exception to this order is the difference between the undecyl and dodecyl homologues of the Py.O*n*O.Py series, which is in fact larger than the corresponding value for the other two series.

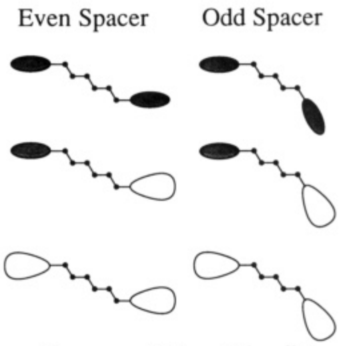

Figure 11. Schematic representation of the all-trans conformation of the dimers; the cyanobiphenyl units are shaded while the pyrene-containing groups are not.

To summarize these observations, therefore, it may be observed that the effect of increasing the biaxiality of the mesogenic groups in dimeric liquid crystals is to reduce the nematic–isotropic transition temperatures while increasing the size of the alternation they exhibit on increasing n. By contrast, the entropy associated with the nematic–isotropic transition and the magnitude of the alternation shown by the entropies as n is varied are both decreased. The asymmetric series has intermediate values of both T_{NI} and $\Delta S_{NI}/R$, but for T_{NI} a positive deviation from linear behavior is observed while for $\Delta S_{NI}/R$ a negative deviation can be seen. Similar though less dramatic effects were reported by Imrie[17] on adding lateral methyl substituents to a series of symmetric dimers. Figure 11 shows a schematic representation of the all-trans conformation for an even and odd member of each series. A number of conformations will be present in the nematic phase, but we consider it instructive to think of the average molecular shape in terms of the all-trans conformation. It is important to note that for an even-membered spacer the two mesogenic units are coparallel, whereas for an odd-membered spacer they form an angle of approximately 108°. Molecular shape is important in determining the liquid-crystalline properties of a compound and to a first approximation the more anisometric the shape, the higher the transition temperatures. It is clear, therefore, that even-membered dimers will, in general, have higher transition temperatures than the odd-membered ones, and this is seen in each of the series discussed here. It is interesting to note that for the analogous monomeric compounds **6** and **7**, the average difference in the clearing points is just

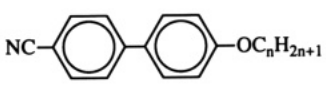

6

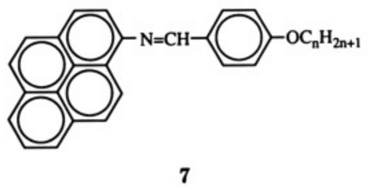

7

---

[17] Imrie, C. T. *Liq. Cryst.* **1989**, *6*, 391.

11 °C,[18,19] whereas for the corresponding dimers it is some 50 °C. This is, in part, a consequence of the change in the molecular symmetry on going from a monomeric structure to a dimeric one. In particular, the molecular long axis for a dimer cannot be considered to be the para axes of the mesogenic units. This accentuates the larger molecular biaxiality of the pyrene moiety and hence lowers the anticipated transition temperatures. The effect of replacing both cyanobiphenyl groups with pyrene-containing moieties is to decrease the shape anisotropy for both even- and odd-membered spacers, resulting in decreased transition temperatures. This effect will be larger in the case of odd-membered spacers in which the cores are not coparallel and hence the transition temperatures of these compounds will be decreased by a greater amount resulting in an increased alternation in the T_{NI}'s. This is indeed the observed behavior. The increased molecular biaxiality acts to also reduce the transitional entropy, and again this is observed experimentally. The alternation in the transitional entropies is more difficult to rationalize, and as noted earlier, it appears that at the root of this effect is an alternation in the long-range orientational order[14] which is difficult to relate to molecular structure. This interpretation of the results predicts that the asymmetric dimers should exhibit the averaged properties of the symmetric dimers; this clearly is not the case. The positive deviation from such behavior exhibited by the transition temperatures is readily explained by the mixed interaction parameter being larger than the geometric mean of the like interaction parameters. The negative deviation from linear behavior shown by the transitional entropies is more difficult to explain, and further discussion must await the result from model calculations which allow for variations in the biaxiality of the mesogenic units.

With the exceptions of the propyl and undecyl homologues, smectic behavior is observed for all the members of the CBO*n*O.Py series, while in the Py.O*n*O.Py series only the hexyl, octyl, and decyl members exhibit smectic phases; for the BCBO*n* series only nematic behavior is observed. This enhancement of the smectic tendencies of the asymmetric dimers almost certainly implies that a specific interaction between the cyanobiphenyl and pyreniminebenzylidene groups exists. Although it is believed that this is a charge-transfer interaction between the electron-poor cyanobiphenyl group and the electron-rich pyreniminebenzylidene group, we cannot exclude the possibility that specific association results from induced dipole–dipole interactions. It is noted that charge-transfer bands are not evident in the UV–vis spectra of dilute solutions in methylene chloride of the asymmetric dimers (see Figure 12), which are simply the sum of the spectra of the two analogous symmetric dimers. It is however possible that such an interaction does occur in a condensed phase such as a mesophase.

Figure 7 also compares the glass transition temperatures exhibited by the Py.O*n*O.Py and CBO*n*O.Py series. Replacing a pyrene unit by a cyanobiphenyl group clearly reduces the glass transition temperature. As has already been noted, the glass-forming ability of the Py.O*n*O.Py series was attributed to the intermolecular face-to-face association of the pyrene groups which leads to the formation of virtual oligomeric or polymeric species[7] although it is surprising to note that the monomeric analogues of these dimers are not reported to form glasses.[18] The dilution of the pyrene–pyrene interactions in the asymmetric dimers accounts for the reduction in the glass transition temperatures. This depression, however, is not as large as may have been anticipated and this reflects the much wider liquid-crystalline temperature ranges exhibited by the asymmetric dimers. Kirov et al.[20] attempted to obtain glassy phases by quenching members of the 4-alkyl-4′-cyanobiphenyl series but even at rates of 50 °C min^{-1} failed to do so. The authors attributed this to the strong dipole–dipole interactions tending to restrict molecular motion, thus favoring crystallization over the formation of a glassy phase. This suggests that for the CBO*n*O.Py series the strong dipole interactions between the cyanobiphenyl groups must be diluted by the mixed-core interaction. However, we should note that Zeller reports a glassy nematic phase for 4-cyano-4′-pentylbiphenyl[21] with an associated glass transition temperature of −63 °C. The ratio of the glass transition temperature to the melting point lies between 0.69 and 0.83 for the Py.O*n*O.Py series and between 0.67 and 0.74 for the CBO*n*O.Py series. For monomeric mesogens this ratio is generally in the range 0.60–0.75[20] while for polymers it is typically around 0.70.[22] This similarity in the T_g/T_m ratios over a wide range of materials indicates that the structural factors determining T_g and T_m are similar.

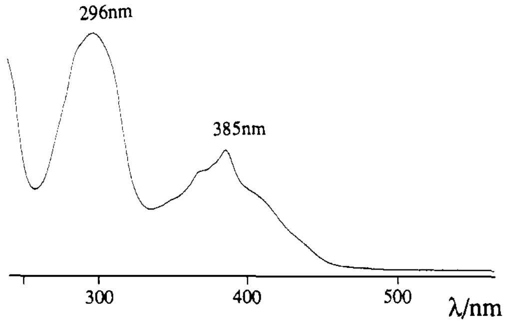

Figure 12. UV–vis spectrum of a dilute solution of CBO7O.Py in methylene chloride.

Glassy low molar mass liquid crystals have considerable application potential in a range of advanced electrooptic technologies. Dimeric materials are particularly attractive as they exhibit high degress of orientational order which has many advantages; for example, it would result in better contrast ratios in optical storage devices. We noted earlier that several members of the asymmetric dimer series crystallized on reheating as in fact do other glassy liquid crystals.[7] However, it must be remembered that in laser-addressed memory storage devices the material is heated and quenched at very high rates, thus preventing crystallization. We have observed no evidence of crystallization below T_g in any of the samples studied here. Finally, we note that the inherent hydrolytic instability of the Schiff's base linkage makes this particular set of materials unsuited to commercial application. They have proved sufficiently stable to permit prolonged physical study at elevated temperatures, and thus they will be of value in the appraisal of this novel class of materials.

Conclusions

Pyrene has been shown to be a valuable group in the design of low molar mass liquid crystals. The effect of

---

[18] Sakagami, S.; Nakamizo, M.; *Kyushu Kogyu Gijutsu Shikensho Hokoku* **1979**, *22*, 1283.

[19] Gray, G. W. In *The Molecular Physics of Liquid Crystals*; Luckhurst, G. R., Gray, G. W., Eds.; Academic Press: New York, 1979; Chapter 1.

[20] Kirov, N.; Fontana, M. P.; Affanassieva, N. *Mol. Cryst. Liq. Cryst.* **1982**, *89*, 193.

[21] Zeller, H. R. *Phys. Rev. Lett.* **1982**, *A26*, 1785.

[22] Karasz, F. E.; Bair, H. E.; O'Reilly, J. M. *J. Polym. Sci., Part A-2* **1968**, *6*, 1141.

pyrene on the transitional properties can be interpreted in terms of the decrease in the molecular shape anisotropy. In addition to the technological potential these materials may prove also to be of interest for time-resolved fluorescence experiments aimed at studying molecular dynamics in anisotropic phases.

Acknowledgment. We are pleased to acknowledge partial support from AFOSR Contract F49620-87-C-0111.

Registry No. 2 ($n = 3$), 143958-46-7; 2 ($n = 4$), 143958-47-8; 2 ($n = 5$), 143958-48-9; 2 ($n = 6$), 143958-49-0; 2 ($n = 7$), 143958-50-3; 2 ($n = 8$), 143958-51-4; 2 ($n = 9$), 143958-52-5; 2 ($n = 10$), 143958-53-6; 2 ($n = 11$), 143958-54-7; 2 ($n = 12$), 143958-55-8; 1-bromo-7-(4-cyanobiphenyl-4′-oxy)heptane, 143958-44-5; 1-(4-cyanobiphenyl-4′-oxy)-7-(4-formylphenyl-4′-oxy)heptane, 143958-45-6.

Synthesis and Second-Order Nonlinear Optical Properties of Polymethacrylates Containing Organic Salt Dye Chromophore

Dong Hoon Choi, Hyun Min Kim, W. M. K. P. Wijekoon, and Paras N. Prasad*

Photonics Research Laboratory, Department of Chemistry, The State University of New York at Buffalo, Buffalo, New York 14214

Received May 8, 1992. Revised Manuscript Received August 17, 1992

New methacrylate polymers containing the *N*-alkylpyridinium salt at the side chain were designed and synthesized in an attempt to enhance both the poling-induced second-order nonlinear optical susceptibility and its temporal stability. The corona poled polymer films showed a large second-order nonlinear optical susceptibility, $\chi^{(2)}(-2\omega;\omega,\omega)$. The larger $\chi^{(2)}$ value of the homopolymer compared to that of the copolymer indicates that the concentration of the nonlinear optical chromophores in the copolymer is lower than the saturation value. The temporal stability of the poled structures seems better than that of some guest–host systems.

Introduction

Side-chain polymers have drawn remarkable interest in recent years as potential candidates for application in electrooptic and photonic devices.[1–6] This interest is partly due to their large optical nonlinearity, relatively high damage threshold, fast response, and high transparency over a wide range of wavelengths. However, one difficulty with second-order organic nonlinear optical (NLO) materials is that most of these compounds crystallize in a centrosymmetric space group and, therefore, even if the microscopic optical nonlinearity, β, may be high, the net bulk susceptibility, $\chi^{(2)}$ vanishes.[1–10] Therefore, the required noncentrosymmetry for a second-order NLO process such as electrooptic effect (EOE) and second harmonic generation (SHG) is usually induced in a polymer by external means of electric field poling. The molecular dipole vector components are aligned by electric poling and subsequent freezing in their new orientation prior to the SHG measurement. Incorporation of NLO molecules to a polymer backbone forming a side-chain NLO polymer backbone forming a side-chain NLO polymer has certain advantages. First, the temporal stability of poled side-chain polymers, in many cases, is better than that of poled guest–host systems.[11–14] Second, a higher concentration of NLO chromophores can be introduced into the polymer matrix to yield a larger second-order optical nonlinearity.

In this paper, we report the synthesis and the second-order NLO behavior of polymers containing a molecular–ionic chromophore, *N*-alkylpyridinium ion, in the side chain. In its powder form, *N*-alkylpyridinium salts have been shown to exhibit significantly high second-order nonlinearities.[15,16] In general, the ionic polymers are difficult to pole because of their intrinsic ionic conductivity. Nevertheless, it has been reported that a significant poling-induced NLO chromophore alignment can be achieved in poled ionic polymers.[17] We show that these molecular

---

(1) *Introduction to Nonlinear Optical Effects in Molecules and Polymers*; Prasad, P. N., Williams, D. J., Eds.; Wiley: New York, 1991.

(2) *Nonlinear Optical Properties of Organic and Polymeric Materials*; Williams D. J., Ed.; ACS Symp. Ser. No. 233; American Chemical Society: Washington, DC, 1983.

(3) *Nonlinear Optical Properties of Organic Molecules and Crystals*; Chemla, D. S., Zyss, J., Eds.; Academic Press: Orlando, FL, 1987.

(4) *Nonlinear Optical Properties of Polymers*; Heeger, A. J., Orenstein, A. J., Ulrich, D. R., Eds.; Mater. *Res. Soc. Symp. Proceedings*, Pittsburgh, 1987; Vol. 109.

(5) *Nonlinear Optical and Electroactive Polymers*; Prasad, P. N., Ulrich, D. R., Eds.; Plenum Press, NY, 1988.

(6) *Organic Molecules for Nonlinear Optics*; Han, R. A., Bloor, D., Eds: The Royal Society of Chemistry Publication: London, 1989; Vol. 69.

(7) Shuto, Y.; Takaara, H.; Mano, M.; Kaino, T. *Jpn. J. Appl. Phys.* **1989**, *28*, 2508.

(8) Mohlmann, G. R.; Horsthuis, W. H. G.; van der Vorst, C. P. M.; Mc Donach, A.; Copeland, M.; Duchet, D.; Fabre, P.; Diemeer, M. B. J.; Trommel, E. S.; Suyten, F. M. M.; van Daele, P.; van Tomme, E.; Baets, R. *Proc. SPIE* **1989**, *1147*, 222.

(9) Haas, D.; Yoon, H.; Man, T.; Cross, G.; Mann, S.; Parsons, N. *Proc. SPIE* **1989**, *1147*, 222.

(10) Singer, K. D.; Holland, W. R.; Kuzyk, M. G.; Wolk, G. L.; Katz, H. E.; Schilling, M. L.; Cahill, P. A. *Proc. SPIE* **1989**, *1147*, 233.

(11) Mortazavi, M. A.; Knoesen, A.; Kowel, S. T.; Henry, R. A.; Hoover, J. M.; Lindsay, G. A. *Appl. Phys. B.* **1991**, *52*, 287.

(12) Hayden, L. M.; Sauter, G. F.; Ore, F. R.; Pasillas, P. L.; Hoover, J. M.; Lindsay, G. A.; Henry, R. H. *J. Appl. Phys.* **1990**, *68*, 456.

(13) Hubbard, M. H.; Marks, T. J.; Yang, J.; Wong, G. K. *Chem. Mater.* **1989**, *1*, 167.

(14) Mandal, B. K.; Chen, Y. M.; Jeng, R. J.; Takahashi, T.; Huang, J. C.; Kumar, J.; Tripathy, S. *Eur. Polym. J.* **1991**, *27*, 735.

(15) Marder, S. R.; Perry, J. W.; Schafer, W. P. *Science* **1989**, *245*, 626.

(16) Kartz, S. K.; Perry, T. T. *J. Appl. Phys.* **1968**, *39*, 3798.

(17) Ye, C.; Mark, T. J.; Yang, J.; Wong, G. K. *Macromolecules* **1987**, *20*, 2322.

0897-4756/92/2804-1253$03.00/0 © 1992 American Chemical Society